Helix Inversions in Polypropylene and Polystyrene

Sergio Brückner*

Dipartimento di Scienze e Tecnologie Chimiche, via Cotonificio 108, 33100 Udine, Italy

Giuseppe Allegra

Dipartimento di Chimica, via Mancinelli 7, 20131 Milano, Italy

Paolo Corradini

Dipartimento di Chimica, Complesso Universitario di Monte Sant'Angelo, via Cintia, 80126 Napoli, Italy

Received October 27, 2001; Revised Manuscript Received February 4, 2002

ABSTRACT: A conformational analysis is done in order to investigate on the mobility of joints separating *d* helical sequences from *l* ones along molecules of polystyrene and polypropylene both isotactic and syndiotactic in solution or in the liquid state. Results indicate that, in the case of isotactic polystyrene, severe interactions between side phenyl rings separated by three and four monomer units play a relevant role in hindering the molecular motions necessary to move the joint. Only a coordinate torsional motion of a number of chain bonds (four) and the overcoming of a rather high energy barrier allows for the motion of the joint along the chain. Syndiotactic polystyrene and iso- and syndiotactic polypropylene show a much easier conformational situation. This may be related to the extreme slowness affecting the crystallization of isotactic polystyrene as compared to the crystallization rate of the other polymers studied. Finally a connection is proposed between results of the present analysis and a possible interpretation of the X-ray diffraction pattern recorded from the oriented (fringed micelle) crystallites contained in crystalline gels of i-PS.

Introduction

Conformations of vinyl polymer chains have been widely investigated both in the crystalline state and in solution.[1−4] They were actually among the first models to be analyzed via computational energy minimization procedures.[5]

In the following, we consider that the actual chiral elements of vinyl polymer chains are the skeletal bonds rather than the carbon atoms, as pointed out by Corradini and Flory.[6,7]

For the bond pair between two tertiary C_α carbon atoms, isotactic chains show two symmetric conformational minima that, upon regular repetition along the chain backbone, may give rise to a right-handed or to a left-handed $3_1/3_2$ helix of equal energy; according to Nagai[1] these two minima are commonly referred to as GT and TG (T = trans and G = ±gauche). More precisely, for the bond pair defined (*d*,*l*) according to Flory's convention[7] or (−,+) according to Corradini's alternative proposal,[6] the minima are TG^+ or G^-T; for the bond pair (*l*,*d*) ≅ (+,−) the minima are TG^-, or G^+T.

Syndiotactic chains show two different conformational minima: TT and GG.[1,2] The GG minimum for the bond pair (d,d) ≅ (−,−) is G^-G^-; for the bond pair (l,l) ≅ (+,+) the minimum is G^+G^+.

In this case too a regular repetition of a sequence such as ...TT GG TT GG... may represent left- or right-handed helices of equal energy, according to the bond chiralities (*l* ≅ + or *d* ≅ −) at the GG pairs.

These conformations are present in the most stable crystalline phases of polypropylene and polystyrene (3_1 helices, with *s*(3/1)1 symmetry, for the isotactic polymers; helices with *s*(2/1)2 symmetry, for the syndiotactic polymers) and in other vinyl polymers.

Conformations near to these of minimum energy are expected to dominate in the random coil state as well; the rotational isomeric state (RIS) approach of Flory, based fundamentally on these models, has allowed for the correct evaluation of the rms end-to-end distance of vinylic polymers[4] and other average configurational properties. If the static average properties of the random coil state of vinylic polymer chains have been well established in relation to their molecular structure, less is known about the influence that intramolecular interactions exert on the dynamical behavior of these polymers, i.e., on their internal viscosity.[8−10]

Isotactic chains are expected to exhibit sequences of right- and left-handed (nearly 3-fold) helices separated by joints where the regularity of the conformational repetition is occasionally interrupted. These joints belong to two different types. With reference to Scheme 1, one of them (type I) is characterized by the side groups being oriented *away* from the joint both in the chain section preceding and in that following the joint. Conversely, in the second type of joint (type II) the side groups are pointing *toward* the joint in both chain sections.[3] It should be stressed that the two joints must always alternate according to the scheme (..I..II..I..II..I..) so that they must occur in equal numbers if the chain is very long. Concerning syndiotactic chains, they are expected to exhibit a succession of trans bonds sequences separated by pairs of gauche rotations.[1,3]

Joints separating different helices undergo thermal equilibration, and therefore, we expect them to display some mobility along the chain backbone; moreover, it is to be noted that they are "annihilated" or "created" always as pairs. Such mobility strongly affects the dynamical behavior of the random coil so that it plays

10.1021/ma0118724 CCC: $22.00
Published on Web 04/12/2002

Scheme 1

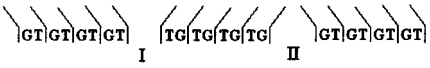

an important role in determining the viscoelastic properties of the polymeric materials; moreover, it becomes particularly important in crystallization processes where only a definite helix is usually allowed to occupy a given crystal site and a chain that is migrating from the amorphous (or solution) phase into the crystalline phase must conform to the stringent requirement of the correct helix chirality and of a well-defined length. For example, including within bars the pair of rotational states around chain bonds located between two consecutive side groups, a ...|TG|TG|TG|.. sequence in an isotactic polymer may be required to change to ...|GT|GT|GT|... (a helix of opposite chirality since for isotactic polymers we adopt the same symbol for a rotation φ on the first bond of the pair as for a rotation $360° - \varphi$ on the second bond, so that G may be either 60 or 300° depending on the location within the pair |XY|). In this case the joint ...|TG|TG|**XY**|GT|GT|..., where X and Y will be specified in a following section, must move to the left, e.g., along the chain backbone until a complete strand of a ...|GT|GT|GT|... helix is deposited on the growing crystal surface. Obviously low mobility of the joint should be reflected into a low rate of crystallization of the polymer.

The present conformational analysis is devoted to the study of the possible chain motions that allow a joint to move along the chain backbone. In particular, we shall focus our attention on the number of bonds that must be driven in order to add a new monomer to a given helical sequence and on the energy barrier that must be overcome in this process. Both features are in fact expected to influence the kinetics of crystallization; the former represents substantially the entropic cost of the transition state whereas the latter represents its enthalpic cost.

Computational Strategy

The study was carried out with the aid of CERIUS[2],[11] a computer program that allows for a wide range of conformational investigations on rather complex molecules.

Isotactic and syndiotactic polypropylene (PP) and polystyrene (PS) were investigated in order to compare the effects of side groups of different encumbrance and those of a different stereoregularity.

Rather long polymer sequences, each spanning 14 monomers, were generated in order to simulate a real polymeric environment near the joint points.

Conformational moves were driven by imposing torsional restraints on selected chain bonds. These restraints act as harmonic potentials whose contributions are to be minimized together with all other force field contributions. For example a torsional angle may be forced to be ϑ_o by imposing the restraint $E_{res} = {}^1/_2K(\vartheta - \vartheta_o)^2$, adding this term to all others and minimizing the overall energy. The value of K can be adjusted so that the restraint acts as an almost rigid constraint or as a weak restriction; both strategies were adopted in our study.

The first and the last three monomeric units in each sequence were strictly ($K = 1000$ kcal/(mol rad^2)) bound to standard values of the helix parameters, to prevent chain-end effects that would tend to distort the regular helix conformation. In some cases weak restraints ($K = 50$ kcal/(mol rad^2)) were instead applied to a number of bonds in the neighborhood of the bonds driven to the conformational transition in order to prevent unwanted conformational changes, that is, conformations drifting away from the range of interest. Molecules in fact become rather unstable as the conformational energy maximum is approached, and it is possible that an uncontrolled bond rotation changes completely its state (e.g., a G may become a T). These changes, after overcoming the energy maximum, are not reversible and a final state is reached that is different from the wanted one. We have introduced restraints that are weak enough to allow for a rather wide conformational flexibility (up to 8−10° from the reference value of the torsional angle) but strong enough to prevent complete conformational transitions. Obviously the energy contribution due to these restraints was subtracted from the total conformational energy.

We point out that all moves reported in this analysis are "real", in the sense that in a conformational transition all atoms move along a continuous trajectory from the starting to the end point, discontinuities being only present in the changes of the restraint values, that were usually incremented by 10° each move. This is an important difference from the usual φ/ψ maps where angle are changed discontinuously, and if angular increments are rather large, it is possible to miss some relevant detail in the conformational path.

We selected the force field indicated as DREIDING 2.21 in the CERIUS[2] program (hereafter DFF force field[12]), a rule-based force field that is suggested for structure predictions and dynamics calculations on organic molecules. A second, rather different, force field, i.e., UNIVERSAL 1.02 (hereafter UFF force field), a rule-based force field applicable to a broad range of the periodic table, validated for organic molecules by Casewit et al.[13] was also used for calculations on i-PS. This was done in order to test the dependence of results on the force fields used in the case of the most critical conformational changes. The reason for choosing DFF and UFF is that they give rise to two different conformations for joint II, namely TA and TT* (see the Results section). This was considered as an indication of a significant difference between the two force fields so that results obtained from both of them could be considered more representative of the uncertainty involved in these calculations.

In both force fields, electrostatic interactions were described by atomic monopoles and charges were attributed to the atoms using the Q_{eq} charge equilibration scheme.[14] A significant difference, among others, between the two force fields, as implemented in CERIUS[2], is in the way the dielectric constant is evaluated in the electrostatic interaction term: UFF uses a fixed value ϵ (we set $\epsilon = 1$) whereas DFF uses a distance dependent value of ϵ ($\epsilon = R_{ij}\epsilon_o$, we set $\epsilon_o = 1$) so that all formal charges in this force field are, actually, reduced by an attenuation factor of $1/\sqrt{R_{ij}}$.

In both cases, a cutoff distance of 4 Å for attractive nonbonded interactions and for Coulombic interactions was selected and a spline function was used, from 4 to 5 Å, to attenuate gradually the interaction energy from its full value to zero. No interaction over 5 Å was taken into account. In this way, we try to avoid the tendency for large molecules to assume contracted conformations only as a result of being considered (in the calculations) in a vacuum and not in a solution or in the liquid state; this is surely appropriate for UFF since ϵ does not increase with distance whereas a smaller effect is expected for DFF. Exploring calculations carried out with a cutoff distance of 8 Å did not show, however, significant differences except, of course, for the absolute value of conformational energies. The minimization algorithm named "smart minimizer" was chosen, which uses a robust but less accurate algorithm near the beginning of the calculation and a less robust but highly accurate one near the end of the run. The convergence criterion adopted was set to very demanding requirements so that, in such complex system, an extremely high number of iterations was necessary to reach convergence. In any case the number of iterations for each conformer was not less than 1000.

Results

Isotactic Polystyrene. This was actually the molecule that required the greatest strategic and compu-

tational effort, the phenyl residue being rigid and protrusive enough to interact strongly with other phenyls that are rather far apart along the chain backbone. Conformational transitions required a severe control of these side groups.

With DFF, two different joints connecting helices of opposite chirality are present:

...|GT|GT|GT|G**T**|**T**G|TG|TG|TG|... (I)

and

...|TG|TG|TG|TG|**TT***|GT|GT|GT|GT|... (IIa)

with its symmetric one

...|TG|TG|TG|TG|**T***T|GT|GT|GT|GT|... (IIb)

Joint I requires less torsional strain whereas joints II involve a higher torsional energy. In any case, it is obvious that both joints must coexist along an isotactic chain since it is reasonable to assume that, in solution or in the melt, a number of helix inversions occur along the same macromolecule.

Alternatively, with the use of UFF, joints IIa and IIb should be indicated as

...|TG|TG|TG|TG|**TA**|GT|GT|GT|GT|... (IIa)

with its symmetric one

...|TG|TG|TG|TG|**AT**|GT|GT|GT|GT|... (IIb)

The difference between joints II is due to intrinsic differences in the two force fields used, a significant shift of the torsion angle from ca. 125° (A) to ca. 155° (T*) is observed, probably due to different parameters describing phenyl−phenyl interactions. One can see, in fact, that a torsion of 155° (flanked by a T) brings two adjacent phenyl rings quite close to each other and in an almost parallel face-to-face fashion. This is allowed by DFF whereas it is not allowed by UFF, and a possible explanation is in the contribution of electrostatic interactions between phenyl rings, since, as already pointed out in the previous section, DFF uses attenuated atomic charges.

This hypothesis was verified by an analysis of the relative stability of TT (or TT*) and TG minima in 2,4-diphenylpentane (DPP). Calculations were performed with the same partial atomic charges reported in Table 1, whereas the dielectric constant ϵ was given different values to check the effect of changing electrostatic interactions. Results are reported in Table 2. It may be seen that UFF and DFF force fields give nearly the same E(TT) − E(TG) in the absence of electrostatic contributions. Increasing charges (i.e., decreasing ϵ) make TG gradually more stable relative to TT (or TT*). The effect is more pronounced with UFF than with DFF, and this may be ascribed to the fact that the two force fields calculate the dielectric constant in different ways. In any case, our analysis indicates that the relative stability of the two minima may be controlled by calibrating the strength of electrostatic interactions, and slightly stronger charges can change the sign of ΔE, making TG more stable than TT. The TA minimum is not stable in DPP, at least with these force fields; therefore, it was not taken into consideration in this analysis; we may expect, however, phenyl−phenyl electrostatic interactions in TA to play a role that is not very different from that played in TG.

Table 1. Parameters for Electrostatic Interactions Used in This Work (According to a Charge Equilibrium Scheme[14]) Compared with Those Used in Ref 15[a]

	charge in elementary charge units	
atom	this work	ref 15
$H(CH_2)$	0.053 (0.0265)	0.18 (0.144)
$C(CH_2)$	−0.106 (−0.053)	−0.16 (−0.15)
C_R	0.0	−0.07 (−0.069)
C_B	−0.127 (−0.0635)	−0.13 (−0.128)
H_B	0.127 (0.0635)	0.14 (0.112)
H(CHR)	0.053 (0.0265)	0.09 (0.072)
C_α(CHR)	−0.053 (−0.0265)	−0.07 (−0.066)

[a] Values in parentheses refer to "effective charges" as result from the attenuation effect due to the dependence of the dielectric constant ϵ on the distance[b] (DFF, this work, see text) and on a more complex algorithm (ref 15) where in addition to the distance, also the chemical nature of interacting atoms is taken into account.[c] [b] Attenuation factor = $1/\sqrt{D_{ij}}$, where an arbitrary D_{ij} distance of 4 Å is assumed. [c] Interactions between equal atoms only, separated by 4 Å, are considered.

Table 2. Conformational Energy Differences E(TG) − E(TT) Computed in 2,4-Diphenylpentane with UFF and DFF Using Different Dielectric Constants (ϵ)[a]

	E(TG) − E(TT) (kcal/mol)	
ϵ	UFF	DFF
∞	2.49	2.43
2	1.55	1.95
1	0.62	1.48

[a] Charges are the same as those reported in Table 1 (second column).

The role played by TT minimum in the conformational features of i-PS has been already discussed by Rapold and Suter[15] in an earlier paper where a substantial prohibition for TT (we call it TT*) conformation was supposed, at variance with previous analyses by Gorin and Monnerie[16] and by Yoon et al.[17] where this conformation was found as a possible state for the molecule. In a more recent paper,[18] dealing with polarization transfer NMR experiments, Suter reconsiders his previous statement and concludes that RIS models without TT fail to account for the measurements on isotactic polystyrene, pointing to a small (5−10%) but significant amount of TT states together with the more abundant trans−gauche needed to agree with the experimental results.

Since, as already shown, electrostatic interactions seem to play an important role in the stabilization of TT* or TA conformational minima, we report in Table 1 the electrostatic charges used by us as compared with those used by Rapold and Suter.[15] DFF, as already stated, uses a variable dielectric constant so that formal charges are actually attenuated by a factor $1/\sqrt{R_{ij}}$; in the second column, in parentheses, we report therefore the DFF "effective" charges belonging to atoms separated by an arbitrary distance of 4 Å (approximately the mean distance between two phenyl rings facing each other). In ref 15, an attenuation factor for electrostatic charges was used too, but it depends, in this case, not only on distances but also on the chemical nature of interacting atoms so that values reported in the second column, in parentheses, refer to interactions between equal atoms separated by 4 Å. It emerges quite clearly that, with DFF, we have used electrostatic charges significantly lower than those used in other calculations.

In this work we are not particularly interested in evaluating the stability of the TT* conformation relative

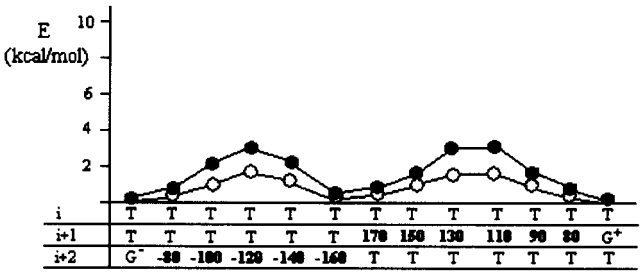

Figure 1. Energy as a function of the conformational path in transition I for i-PS. Open circles represent the torsional contribution. Bold numbers indicate torsion angles imposed as strong restraints; T and G symbols indicate the corresponding rotational states trans and ±gauche but allow for wide deviations (up to 20°) from standard values.

Scheme 2

$$|GT|GT|GT|GT|GT|GT|G_{i-1}\mathbf{T}_i|\mathbf{T}_{i+1}G_{i+2}|TG|TG|TG|TG|TG|TG|$$

$$\downarrow \text{Transition I}$$

$$|GT|GT|GT|GT|GT|GT|G_{i-1}T_i|G_{i+1}\mathbf{T}_{i+2}|\mathbf{TG}|TG|TG|TG|TG|TG|$$

to other conformational minima, as we simply consider it (together with TA) as a necessary event once the alternation of right- and left-handed helices along the same isotactic macromolecule is accepted. In fact, as recognized already by Rapold and Suter, the rigorous prohibition of *meso* TT states would imply the existence of a single "break" (we call it a joint) between two helices of opposite chirality along the same macromolecule, thus leading to the calculation of very high characteristic ratios, for isotactic polystyrene, contrary to experiment. We accept instead the point of view that a significant number of joints connecting different helices on the same chain are present in the melt or in solution of that polymer.

Let us indicate as transition I the conformational change that shifts joint I of two bonds (one monomer unit) along the chain (Scheme 2). The transition involves changes on bonds $i + 1$ and $i + 2$; it may be driven in one step provided bond $i + 2$ is driven first (G → T) and bond $i + 1$ is driven last (T → G). Bond i was weakly restrained to be trans throughout the transition because otherwise, near the first barrier, it would tend to change to gauche. Results are shown in Figure 1 where the overall energy E is plotted as a function of the torsional angles around bonds i, $i + 1$ and $i + 2$. Bold numbers indicate the angular values of a strongly driven torsion whereas T and G symbols indicate the respective rotational states, sometimes with a rough approximation (±20°). Bond $i + 2$ was first driven to T, and then it was left uncontrolled while bond $i + 1$ was driven to G^+. A double barrier is observed with maxima near the anticlinal conformations of the two bonds, the highest maximum is ca. 3.5 kcal/mol. We report also, as open circles, the torsional contribution to the total energy.

A similar calculation was carried out with UFF with rather similar results; a double barrier was again observed at angular values similar to those reported in Figure 1, and the highest maximum was ca. 6 kcal/mol. We do not show the figure for brevity, since it does not imply a significant difference relative to Figure 1. In Figure 2 we show the starting (a) and the final (c) states together with an intermediate state (b) near the first energy barrier.

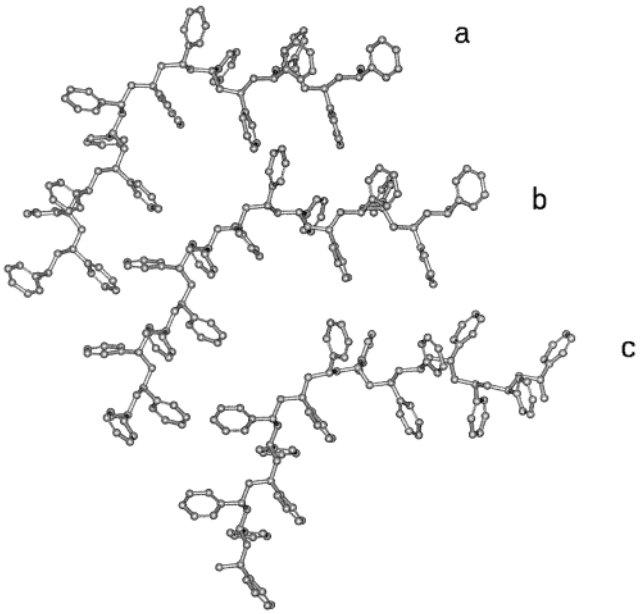

Figure 2. Molecular models of i-PS involved in transition I: the starting model (a), the final model (c), and an intermediate model (b) recorded near the energy maximum.

Scheme 3

$$|TG|TG|TG|TG|TG|TG|T_{i-1}T^*_i|G_{i+1}T_{i+2}|GT|GT|GT|GT|GT|GT|$$

$$\downarrow \text{Transition II}$$

$$|TG|TG|TG|TG|TG|TG|T_{i-1}G_i|T_{i+1}T^*_{i+2}|GT|GT|GT|GT|GT|GT|$$

Scheme 4

$$|TG|TG|TG|TG|TG|\underset{*}{TG}|T_{i-1}T^*_i|G_{i+1}T_{i+2}|GT|\underset{*}{GT}|GT|GT|GT|GT|$$

$$\downarrow \text{Transition II, step 1 (bonds i, i+1)}$$

$$|TG|TG|TG|TG|TG|TG|T_{i-1}G_i|T^*_{i+1}T_{i+2}|GT|GT|GT|GT|GT|GT|$$

Scheme 5

$$|TG|TG|TG|TG|TG|\underset{*}{TG}|T_{i-1}G_i|T^*_{i+1}T_{i+2}|GT|\underset{*}{GT}|GT|GT|GT|GT|$$

$$\downarrow \text{Transition II, step 2 (bonds i+1, i+2)}$$

$$|TG|TG|TG|TG|TG|TG|T_{i-1}G_i|T_{i+1}T^*_{i+2}|GT|GT|GT|GT|GT|GT|$$

We indicate as transition II the conformational change that shifts joint II of two bonds along the chain: The transition involves changes on three bonds, i.e., bonds i, $i + 1$, and $i + 2$.

In this case, some phenyl groups play an important role and make the transition very difficult. First of all it is expedient to separate the transition into two steps, each involving two bonds (Schemes 4 and 5). One can see that step 1 corresponds to a change from one joint to the symmetric one (on the next monomer) and step 2 to a reverse change on the same monomer; the overall result is a shift of the joint to the next monomer.

In step 1 (Scheme 4) the phenyl groups located at the two starred positions conflict with each other so that the transition cannot occur by simply driving bond i and bond $i + 1$ from their initial to their final values. If one forces, in this way, the model to the new conformation, a high energy state is obtained which, upon release of the restraints, returns to the starting model, so that no conformational transition takes place. The transition can occur only if additional bonds are properly driven

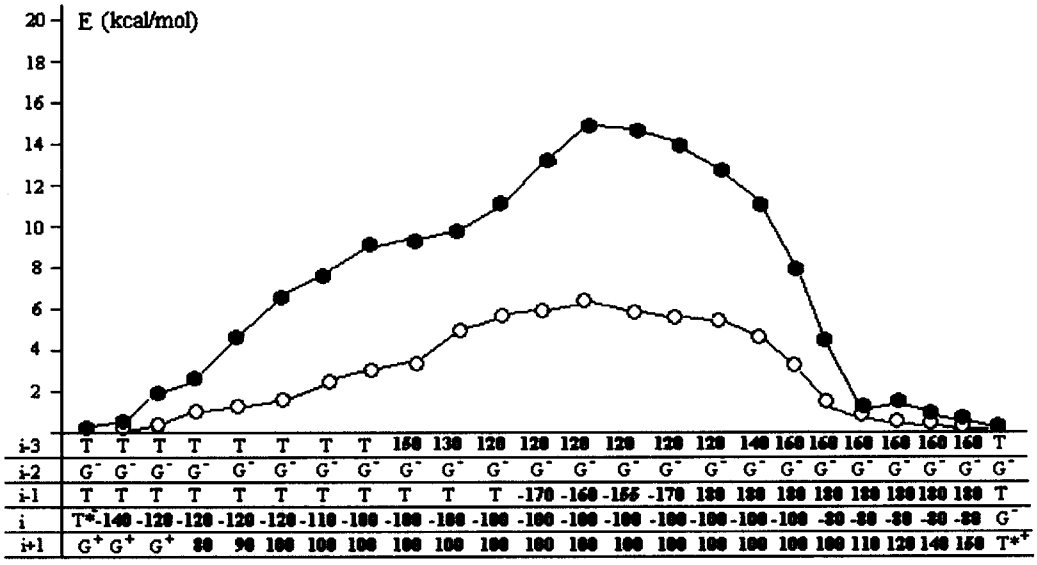

Figure 3. Energy (black circles) as a function of the conformational path in transition II (step 1) for i-PS. Open circles represent the torsional contribution to the total energy. Bold numbers indicate torsion angles imposed as strong restraints; T, G and A symbols indicate the corresponding trans, ±gauche, and ±anticlinal states but allow for wide deviations from standard values.

so that the two phenyl groups can avoid each other during the conformational change. There is no unique way to obtain this result since many bonds separate the two phenyls (eight chain bonds + two side bonds) and numerous combinations of torsional angles on these bonds can reach the objective of releasing interactions between these side groups. We have tried some possibilities and have selected the transition that leads, in our calculations, to the least energy barrier.

In Figure 3, we report the energy as a function of the conformational path in step 1 using DFF. In addition to bonds i and $i + 1$ two more bonds must be driven; we found it most convenient to act on bonds $i - 1$ and $i - 3$, whereas bonds $i - 2$, $i + 2$, and $i + 3$ were weakly bonded to their starting torsion angle. One can see that in the neighborhood of the maximum energy all four bonds are driven simultaneously.

An energy barrier of ca. 15 kcal/mol is computed. A comparison with the torsional contribution (open circles) shows the relevant role played, in this case, by nonbonded interactions, an effect that is mainly due to side phenyl groups.

In Figure 4, we show the starting (a) and the final (c) states together with an intermediate (b) state near the energy maximum; the two phenyl rings most involved in the conformational transition are evidenced as black rings.

In step 2 (Scheme 5), two phenyls are again strongly involved, they are in the starred positions reported in the scheme, and one can see that now they are separated by 12 bonds (10 chain bonds + 2 side bonds) thus increasing the number of possible conformational paths suitable to release the steric conflict between them. We have found a trial path that involves three bonds and keeps the energy barrier relatively low and report it in Figure 5.

In addition to bonds $i + 1$ and $i + 2$, one more bond had to be driven; we found it most convenient to act on bond $i - 1$, whereas bonds i, $i - 2$, and $i + 3$ were weakly bonded to their starting torsion angle. An energy barrier of ca. 9 kcal/mol was computed, lower than that of step 1, and this is reasonable considering that the strain

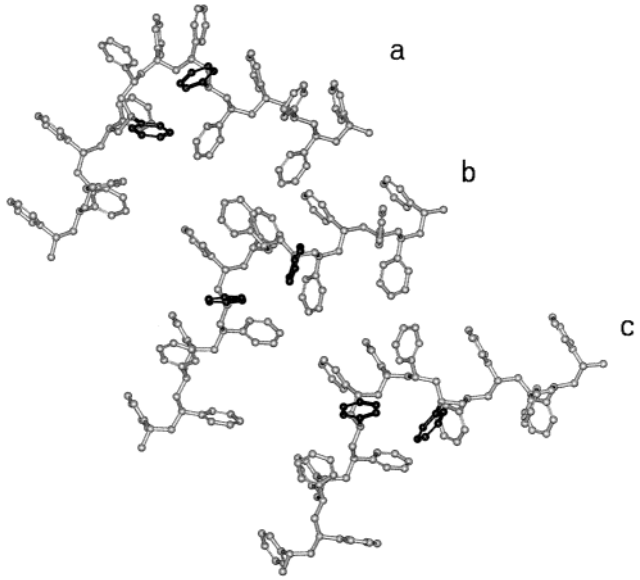

Figure 4. Molecular models of i-PS involved in transition II (step 1): the starting model (a), the final model (c), and an intermediate model (b) recorded near the energy maximum.

required to keep apart the two phenyls may now be distributed over a greater number of bonds.

In Figure 6 we show the starting (a) and the final (c) states together with an intermediate (b) state recorded near the energy maximum; the two phenyls most involved in the conformational transition are again depicted as black rings.

A similar calculation was performed with UFF according to Schemes 6 and 7. As already discussed, the difference is mainly represented by the conformational minimum at TA instead of TT*, due to the different force field used. The physical obstacle to the conformational change, represented by the two phenyl rings at the starred positions, obviously remains the same, and again a conformational path had to be found that alleviates these interactions, just like the previous analysis. Step 1 required a higher energy barrier of 18 kcal/mol, due to the fact that UFF treats phenyl−phenyl

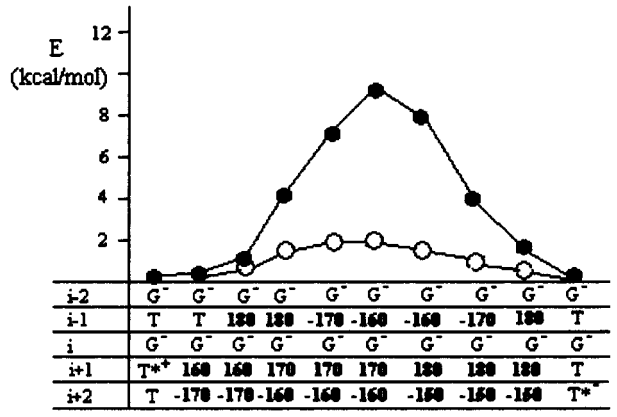

i-2	G⁻	G⁻	G⁻	G⁻	G⁻	G⁻	G⁻	G⁻	G⁻	G⁻
i-1	T	T	180	180	-170	-160	-160	-170	180	T
i	G⁻	G⁻	G⁻	G⁻	G⁻	G⁻	G⁻	G⁻	G⁻	G⁻
i+1	T*⁺	160	160	170	170	170	180	180	180	T
i+2	T	-170	-170	-160	-160	-160	-160	-160	-160	T*⁻

Figure 5. Energy as a function of the conformational path in transition II (step 2) for i-PS. Open circles represent the torsional contribution to the total energy. Bold numbers indicate torsion angles imposed as strong restraints; T, G, and A symbols indicate the corresponding trans, ±gauche, and ±anticlinal states but allow for wide deviations from standard values.

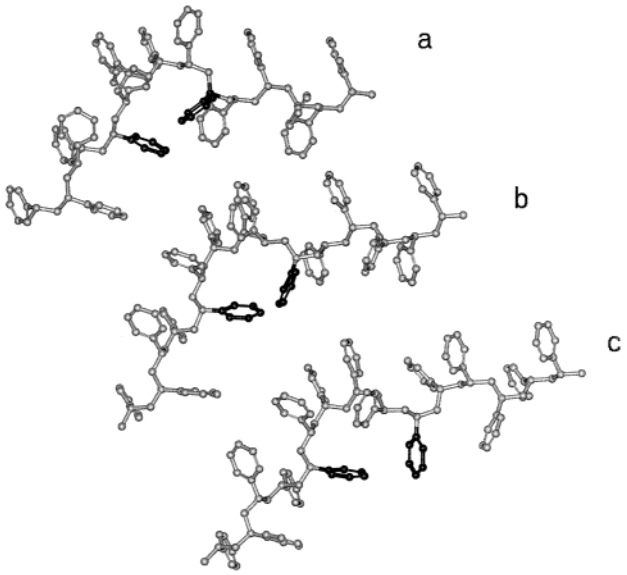

Figure 6. Molecular models of i-PS involved in transition II (step 2): the starting model (a), the final model (c), and an intermediate model (b) recorded near the energy maximum.

Scheme 6

$$|TG|TG|TG|TG|\underset{*}{TG}|TG|T_{i-1}A_i|G_{i+1}T_{i+2}|GT|\underset{*}{GT}|GT|GT|GT|GT|$$

$$\downarrow \text{Transition II, step 1 (bonds i, i+1)}$$

$$|TG|TG|TG|TG|TG|TG|T_{i-1}G_i|A_{i+1}T_{i+2}|GT|GT|GT|GT|GT|GT|$$

Scheme 7

$$|TG|TG|TG|TG|\underset{*}{TG}|\overset{i-1\ i\ \ i+1\ i+2}{TG|T_{i-1}G_i|A_{i+1}T_{i+2}}|GT|\underset{*}{GT}|GT|GT|GT|GT|$$

$$\downarrow \text{Transition II, step 2 (bonds i+1, i+2)}$$

$$|TG|TG|TG|TG|TG|TG|T_{i-1}G_i|T_{i+1}A_{i+2}|GT|GT|GT|GT|GT|GT|$$

interactions in a more severe way, and again four bonds had to be simultaneously controlled to perform the conformational change. Unlike the previous analysis, step 2 required four bonds to be simultaneously controlled, and an energy barrier of ca. 13 kcal/mol was computed.

Scheme 8

$$|GG|TT|GG|TT|GG|TT|TT_{i-1}|G_iG_{i+1}|T_{i+2}T|GG|TT|GG|TT|GG|$$

$$\downarrow$$

$$|GG|TT|GG|TT|GG|TT|GG_{i-1}|T_iT_{i+1}|T_{i+2}T|GG|TT|GG|TT|GT|$$

Syndiotactic Polystyrene. In syndiotactic polystyrene we have considered one joint

$$|GG|TT|GG|TT|GG|\mathbf{TT}|\mathbf{TT}|GG|TT|GG|TT|GG|TT|GG|$$

where |TT|TT| connects two helices of opposite chirality. The conformational transition shown in Scheme 8 was studied. It corresponds to the transition of two monomeric units from one helix to the opposite one.

In this case, the transition did not involve strong conflicts among side groups, and it was possible to perform it by driving the four bonds one at a time without the cooperative changes of other bonds.

It was only necessary to put a weak restraint on bond $i - 1$ when bond i was first driven from G to T; otherwise, it tends to change to G.

Bonds were driven following the order: i first, $i + 1$ second, $i - 1$ third, and $i - 2$ last. This was done in order to avoid the presence of G^+G^- pairs that involve strong repulsion effects; no additional restraint was necessary. Energy as a function of the conformational path is reported in Figure 7. An energy barrier of ca. 6.5 kcal/mol (first barrier) was computed, and the absolute minimum was found to be in correspondence with the intermediate state where eight adjacent bonds are in the trans conformation. Open circles show the torsional contribution to the total energy; it may be seen that each bond contributes separately to this term.

In Figure 8, we show the starting (a) and the final (c) states together with the intermediate state (b).

Use of UFF in the calculation led to an energy barrier of ca. 11 kcal/mol and changed the absolute minimum position since the intermediate state, with eight bonds in the trans state, was ca. 4 kcal higher than the starting state.

Isotactic and Syndiotactic Polypropylene. Conformational changes in polypropylene were by far less difficult to perform than those in polystyrene. The side methyl group exerts an important influence only on the immediate neighbor monomers, but it is not enough protrusive to interact with groups located on farther monomers.

In isotactic polypropylene, transitions I and II are formally equal to the analogous transitions described in isotactic polystyrene (see previous schemes).

Energy as a function of the conformational path for transition I is shown in Figure 9. Bond $i + 2$ is driven first and bond $i + 1$ is driven last; no additional restraint was necessary. An energy barrier of ca. 4 kcal/mol is computed.

The conformational path of transition II, comprising both step 1 and step 2, is reported in Figure 10. The two steps appear as two barriers, the higher being of ca. 3.5 kcal/mol. In this case too no additional restraint was necessary and it may be seen that, at maximum, only two bonds were simultaneously driven. In this case, differences between DFF and UFF are really small, and no systematic comparison has been carried out.

In the case of syndiotactic polypropylene, we analyzed the same transition as in polystyrene (see Scheme 8), and again the transition could be performed by driving

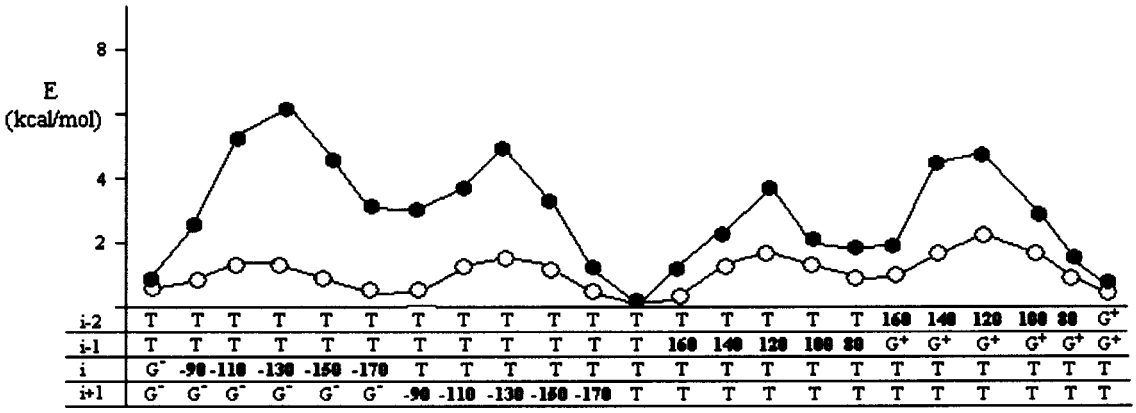

Figure 7. Energy as a function of the conformational path for s-PS. Open circles represent the torsional contribution to the total energy. Bold numbers indicate torsion angles imposed as strong restraints; T and G symbols indicate the corresponding trans and ±gauche states but allow for wide deviations from standard values. Note that bonds are driven one at a time.

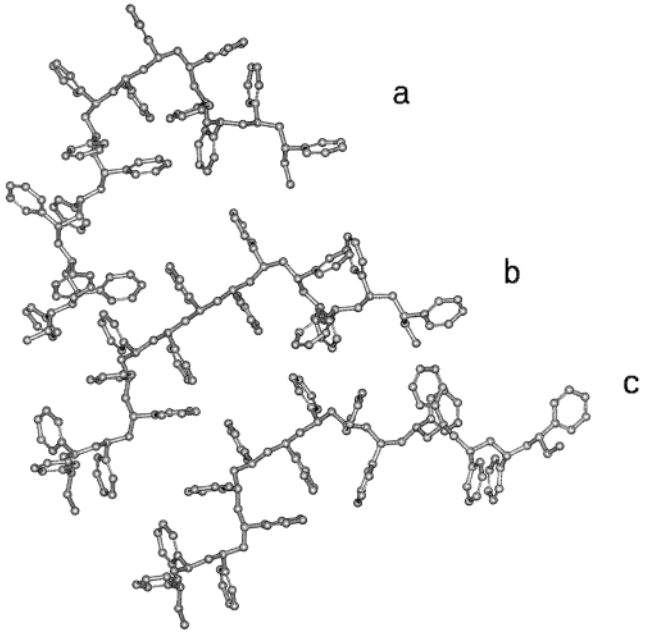

Figure 8. Molecular models of s-PS: the starting model (a), the final model (c), and an intermediate model (b) recorded at the relative minimum corresponding to eight successive T states.

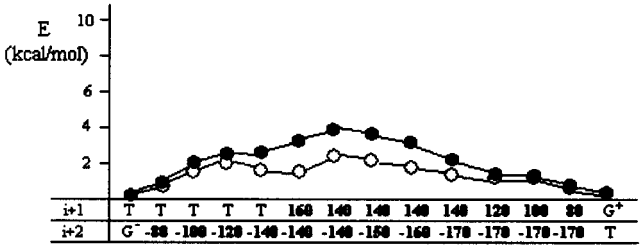

Figure 9. Energy as a function of the conformational path in transition I for i-PP. Bold numbers indicate torsion angles imposed as strong restraints; T and G symbols indicate the corresponding rotational states trans and ±gauche but allow for wide deviations from standard values.

one bond at a time without the need to control other bonds. Results are reported in Figure 11 where two energy barriers are visible of approximately the same height (ca. 5 kcal/mol). Unlike polystyrene, the intermediate state of eight adjacent bonds in the trans conformation appears to be as stable as the helix.

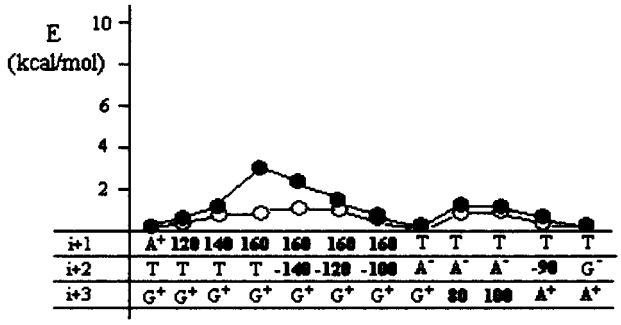

Figure 10. Energy as a function of the conformational path in transition II (both steps) for i-PP. Bold numbers indicate torsion angles imposed as strong restraints; T, G and A symbols indicate the corresponding rotational states trans, ±gauche, and ±anticlinal but allow for wide deviations from standard values.

Discussion and Concluding Remarks.

First of all we want to emphasize the semiquantitative character of the results obtained in this study. Molecular mechanics is actually a well-founded approach, and data obtained with this methodology are reliable; however, the problem studied here is rather complex since a great number of variables must be taken into account and some arbitrariness and approximations are necessary.

As a first remark, nonnegligible differences depend on the choice of the force field to be used in the calculations. We draw a comparison between two different force fields, i.e., DFF and UFF, and results may give an idea of the uncertainty affecting our data due to this kind of choice. This is particularly evident in the case of PS. We also point out the very general point that force fields are commonly developed to faithfully locate energy minima, not maxima. Some uncertainty may therefore affect energy contributions due to highly strained geometries.

As a second remark, we point out that only a limited number of possible paths for the conformational changes have been actually explored. A systematic analysis and energy optimization of the possible cooperative motions of about 10 torsion angles to obtain all possible paths leading from one given starting conformation to the final one is a heavy task even with the help of a powerful computer. This means that, particularly for i-PS, the number and kind of bonds involved in the conformational transitions, and the resulting energy barriers, are

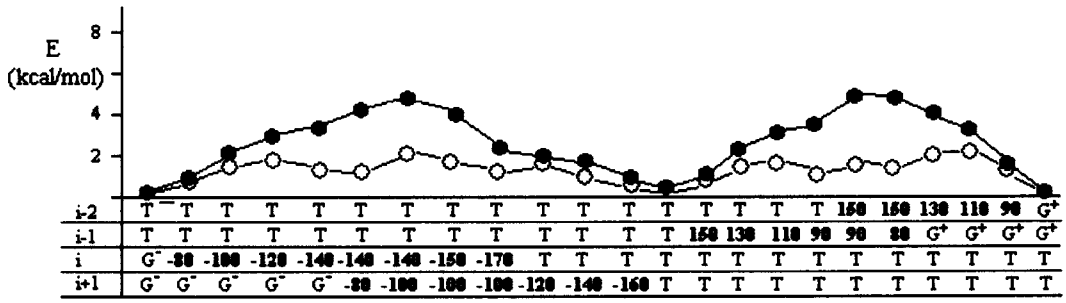

Figure 11. Energy as a function of the conformational path s-PP. Bold numbers indicate torsion angles imposed as strong restraints; T and G symbols indicate the corresponding rotational states trans and ±gauche but allow for wide deviations from standard values.

Table 3. Results of the Present Conformational Analysis

polymer	energy barrier (kcal/mol)	no. of simultaneously driven bonds
i-PS (step 1)	15	4
i-PS (step 2)	9	3
s-PS	6.5	1
i-PP	4	2
s-PP	5	1

to be regarded as possible examples of what may actually happen in conformational changes.

Having established these limitations, we can discuss however some aspects that are, in our opinion, significant and make our study meaningful.

The point that emerges quite clearly, and is not influenced by the aforementioned limitations, is that conformational changes involving polystyrene, in particular i-PS, are strongly influenced by side phenyl groups that are separated by 8−10 bonds along the polymer chain. A side group such as methyl, that is, locally, as cumbersome as phenyl but definitely less protrusive, plays a much less critical role, as results from the analogous conformational transitions of polypropylene, where a lower energy barrier is computed and a maximum of two bonds are required to undergo cooperative changes (see Table 3). This means that significant results concerning helix inversion in i-PS cannot be reached unless rather long chain sequences, on the order of at least five to six monomeric units, are taken into account.

Results are summarized in Table 3. A big difference appears immediately between isotactic polystyrene and the other chains studied. In particular, transition II, as already stated, requires the simultaneous control of four bonds and presents an energy barrier of ca. 15 kcal/mol. This suggests immediately a substantial difficulty for this polymer to display mobility of joints II connecting two opposite helix sequences. Transition I appears to be less critical but this does not influence the overall phenomenon since it is clearly governed by the slowest process, which is the reason for omitting the corresponding results in Table 3.

Syndiotactic polystyrene presents a lower energy barrier (ca. 9 kcal/mol) where the conformational transition can be performed by driving one bond at a time, and this makes the move much less critical than the preceding one, so no particular cooperation is in fact required among adjacent torsional states in order to accomplish the transition. Results are also more reliable since the possibility of driving one bond at a time allows the other bonds to adjust to the minimum of conformational energy at every step of the conformational change.

As an additional remark concerning isotactic and syndiotactic polystyrene, we point out that the higher degree of bond-rotation cooperativity required in the former polymer to obtain the transitions under investigation implies a higher entropy barrier, which makes the energy barrier difference even larger than discussed previously.

In conclusion, the mobility of joints connecting helices of opposite chirality appears to be very low for i-PS and significantly higher for s-PS.

Polypropylene, both isotactic and syndiotactic, displays energy barriers that are definitely much lower than those encountered in polystyrene and changes that may be driven by controlling a maximum of two bonds in the case of i-PP.

In the case of PP, differences between i-PP and s-PP are not so relevant, and no apparent reason exists to predict a greater mobility of the joints connecting helices of opposite chirality in one polymer rather than in the other.

Rate of crystallization seems to be a natural matter of comparison for these data since, as already stated in the Introduction, the deposition of a random coiled chain on the crystal surface that requires an helix of given chirality and given length must be accompanied by such conformational transitions as those depicted in this analysis. This comparison must be done, however, by keeping in mind that the conformational moves studied by us are only part of the whole crystallization process; in fact we do not account at all for very important contributions to crystallization kinetics like, for example, molecular diffusion effects, in the implicit assumption that this factor by itself should not reverse the present conclusions. Therefore, all comparisons will be kept at a semiquantitative level.

The difficulty of i-PS to crystallize both from solution and from the melt is well-known. An example of comparison between the crystallization rate constants of i-PS and s-PS is found in a paper by Haneda et al.[19] where a factor on the order of ca. 10^{-8} exists, at 210 °C, between the two rate constants. In the same paper the activation energy for s-PS crystallizing from the melt is found to change from 12 to 20 kcal/mol at increasing molecular weight from 3.5×10^5 to 2×10^6. Our data are lower and, obviously, independent from molecular weight being only interested in very local motions of an isolated fragment. As already stated, these data confirm that more general motions must be involved in the real crystallization process, but, nevertheless, we must emphasize that our analysis may give a satisfactory explanation, at a molecular level, of the extreme difficulty of i-PS in crystallizing.

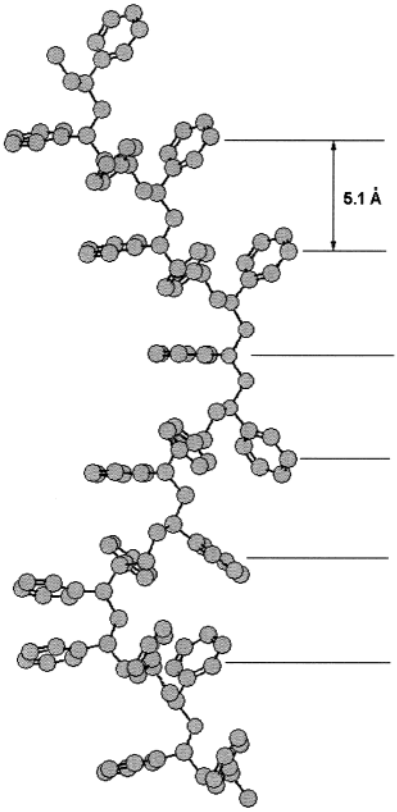

Figure 12. Model giving the possible explanation of the meridional reflection of 5.1 Å occurring in oriented crystalline gels of isotactic polystyrene.

We note finally that the results obtained in this paper for the minimum energy conformations at the joints of 3-fold helices of opposite chirality for isotactic polystyrene, i-PS, open the possibility to build models with extended chains of the kind ...$(TG)_{3m}(TT)(GT)_{3n}(TG)_{3p}$-$(TT)(GT)_{3q}$.... with m, n, p, and q integers, which could be the precursors of the more regular conformations, which give rise to the classical meridional reflection at 5.1 Å from the oriented (fringed micelle) crystallites contained in crystalline gels of i-PS (the 5.1 Å meridional reflection would correspond locally to the span of three monomeric units, instead of two, as previously supposed (see Figure 12)). In such gels, at variance with the previously proposed models having helices of a single chirality,[20−22] Auriemma et al. have in fact proposed recently[23] that short stretches of right- and left-handed helices succeed each other regularly along the chain axis, to give the observed repetition period of 30.6 Å (for example sequences such as $(TG)_6(TT)(GT)_9$ give an i-PS chain having 16 monomeric units within a period $c \cong 30.6$ Å).

In syndiotactic polypropylene, it has been observed that TTGG helical successions may be broken by long even sequences of TT conformations (such as ...TTGG-$(TT)_{2n}$TTGG..., $n = 0, 1, 2, ...$) to give kink bands,[24] across which the helices have the same sense of spiralization or by long odd sequences of TT conformations (such as ...TTGG$(TT)_{2n+1}$TTGG..., $n = 0, 1, 2, ...$) across which the helices change their sense of spiralization. We note that inversions in the sense of spiralization along one single chain, as considered in this paper, may occur also inside of crystals as components of localized defects or at their surface in the folds.

Acknowledgment. The authors are grateful to INSTM (Consorzio Interuniversitario Nazionale per la Scienza e Tecnologia dei Materiali)−Computational Initiative for having made available program CERIUS[2] to its members. Financial support from the "Ministero della Ricerca Scientifica e Tecnologica" is gratefully acknowledged (P.C.).

References and Notes

(1) Nagai, K. *J. Chem. Phys.* **1959**, *30*, 660; **1959**, *31*, 1169.
(2) Natta, G.; Corradini, P.; Ganis, P. *Makromol Chem.* **1960**, *39*, 238.
(3) Corradini, P.; Allegra, G. *Rend. Acc. Naz. Lincei*, *Rend. Cl. Sci. Fis. Mat. Nat.* (8) **1961**, *30*, 516. Allegra, G.; Ganis, P.; Corradini, P. *Makromol. Chem.* **1963**, *61*, 225.
(4) Flory, P. J.; Mark, J. E.; Abe, A. *J. Am. Chem. Soc.* **1966**, *88*, 639. Flory, P. J. *J. Am. Chem. Soc.* **1967**, *89*, 1798.
(5) Suter, U. W.; Flory, P. J. *Macromolecules* **1975**, *8*, 765.
(6) Corradini, P. *The stereochemistry of Macromolecules*; Ketley, A. D., Ed.; Marcel Dekker: New York, 1968; Vol. 3, pp 2−9.
(7) Flory P. J. *Structural Order in Polymers*; Ciardelli, F., Giusti, P., Eds.; Pergamon Press: Oxford, England, 1981; pp 5−7.
(8) Peterlin, A. *J. Polym. Sci.* **1967**, *A-2 5*, 179.
(9) Cerf, R. *J. Polym. Sci.* **1967**, *23*, 125.
(10) Allegra, G. *J. Chem. Phys.* **1974**, *61*, 4910. Allegra, G.; Ganazzoli, F. *Macromolecules* **1981**, *14*, 1110. Allegra, G.; Ganazzoli, F. *Adv. Chem. Phys.* **1989**, *75*, 265.
(11) Cerius[2] Modeling Environment, Month 1999. Molecular Simulations Inc.: San Diego, CA, 1999.
(12) Mayo, S. L.; Olafson, B. D.; Goddard, W. A., III *J. Phys. Chem.* **1990**, *94*, 8897.
(13) Casewit, C. J.; Colwell, K. S.; Rappé, A. K. *J. Am. Chem. Soc.* **1992**, *114*, 10035.
(14) Rappé, A. K.; Goddard, W. A., III *J. Phys. Chem.* **1991**, *95*, 3358.
(15) Rapold, R. F.; Suter, W. *Macromol. Theory Simul.* **1994**, *3*, 1.
(16) Gorin, S.; Monnerie, L. *J. Chim. Phys.* **1970**, *67*, 869.
(17) Yoon, D. Y.; Sundararajan, P. R.; Flory, P. J. *Macromolecules* **1975**, *8*, 776.
(18) Robyr, P.; Gan, Z.; Suter, U. W. *Macromolecules* **1998**, *31*, 8918.
(19) Haneda, T.; Hashima, Y.; Tanaka, Y. *Rep. Prog. Polym. Phys. Jpn.* **1989**, *32*, 107.
(20) Sundararajan, P. R. *Macromolecules* **1979**, *12*, 575.
(21) Atkins, E. D. T.; Isaac, D. H.; Keller, A. *J. Polym. Sci., Polym. Phys. Ed.* **1980**, *18*, 71.
(22) Keller, A. *Faraday Discuss.* **1995**, *101*, 1.
(23) Auriemma, F.; De Rosa, C.; Vinti, V.; Ricciardi, R.; Corradini, P. 2nd International Conference on Polymer−Solvent Complexes and Intercalates, Ischia, Italy. *Commun. Prepr.* **1998**, 48−49.
(24) Auriemma, F.; De Rosa, C.; Ruiz de Ballestreros, O.; Corradini, P. *Macromolecules* **1997**, *30*, 6586.

MA0118724